RSC Advances

PAPER

View Article Online
View Journal | View Issue

Cite this: *RSC Adv.*, 2019, **9**, 13254

In vitro cytotoxicity and antibiotic application of green route surface modified ferromagnetic TiO_2 nanoparticles

A. K. M. Atique Ullah, *[ab] A. N. Tamanna,[c] A. Hossain,[d] M. Akter,[e] M. F. Kabir,[c] A. R. M. Tareq,[f] A. K. M. Fazle Kibria,[g] Masaaki Kurasaki,[e] M. M. Rahman[c] and M. N. I. Khan[h]

The enormous numbers of applications of TiO_2 nanoparticles (NPs) cause concern about their risk to the environment and human health. Consequently, motivated by the necessity of searching for new sources of TiO_2 NPs of low cytotoxicity with antibacterial activity, we synthesized TiO_2 NPs by a green route using a solution of titanium(IV) isopropoxide as a precursor and an aqueous extract of *Artocarpus heterophyllus* leaf as a reducing and surface modifying agent. We investigated their structure, shape, size, and magnetic properties, and evaluated their antibiotic application and cytotoxicity. The synthesized TiO_2 NPs were applied against two Gram-negative bacteria (*E. coli* and *S. typhimurium*) and two Gram-positive bacteria (*S. aureus* and *B. subtilis*) to observe their antibacterial activity; and eventually clear zones of inhibition formed by the TiO_2 NPs were obtained. Moreover, after exposing the synthesized TiO_2 NPs to HeLa cells (carcinoma cells) and Vero cells (normal cells), no toxic effect was found up to a dose of 1000 mg L^{-1}, indicating the safe use of the samples up to at least 1000 mg L^{-1}. However, toxic effects on HeLa cells and Vero cells were observed at doses of 2000 mg L^{-1} and 3000 mg L^{-1}, respectively. These results indicate the safe use of *Artocarpus heterophyllus* leaf extract mediated synthesized TiO_2 NPs in their potential applications.

Received 25th February 2019
Accepted 15th April 2019

DOI: 10.1039/c9ra01395d

rsc.li/rsc-advances

Introduction

Titanium dioxide (TiO_2) NPs have wide applications in dye sensitized solar cells and the purification of air and water due to their potential oxidation strength, high photo stability, and non-toxicity.[1–3] TiO_2 NPs also possess interesting optical, dielectric, antimicrobial, antibacterial, chemical stability, and catalytic properties, which lead to industrial applications such as pigments, paints, toothpaste, fillers, catalyst supports, photocatalysts, gas sensors, and optoelectronic devices.[4–8] This enormous number of applications of TiO_2 NPs may result in the absorption of NPs through the lung or gastrointestinal tract into systematic circulation and then their distribution to different organs, such as the liver, kidneys, spleen, or even the brain, causing localized effects.[9]

The anatase phase of the TiO_2 crystal exposes low energy, thereby minimizing the surface energy and increasing the crystal stability.[10] In addition, the anatase phase is chemically and optically active and hence it is suitable for use as a catalyst and as a support.[11] The functionality of NPs depends on various factors and among them size, shape, morphology, and crystallinity are notable in depending on the mode of synthesis.[12–14] TiO_2 NPs have been synthesized by using sol–gel, microemulsion, chemical precipitation, hydrothermal, solvothermal, electrochemical, and biological synthesis methods.[15] Among all these methods, the green synthesis of nanomaterials, usually known as bio-synthesis, is gaining attention from researchers because of its simplicity, speed, non-toxicity, and economical approach.[16] Bio-syntheses of NPs by bacteria, fungi, yeast, or plant extracts are the best alternatives to develop cost-effective, less laborious, non-toxic, and environmentally friendly NPs for avoiding adverse effects in many nanomaterial applications.[17] The synthesis of NPs using plant extracts is more effective than using microbes, because the presence of biomolecules in plants

[a]*Nanoscience and Technology Research Laboratory, Atomic Energy Centre, Bangladesh Atomic Energy Commission, Dhaka 1000, Bangladesh. E-mail: atique.chem@gmail.com; atique.chem@baec.gov.bd*

[b]*Analytical Chemistry Laboratory, Chemistry Division, Atomic Energy Centre, Bangladesh Atomic Energy Commission, Dhaka 1000, Bangladesh*

[c]*Department of Physics, University of Dhaka, Dhaka 1000, Bangladesh*

[d]*Department of Physical and Inorganic Chemistry, Institute of Natural Sciences and Mathematics, Ural Federal University, 620000 Yekaterinburg, Russia*

[e]*Graduate School of Environmental Science, Hokkaido University, 060-0810 Sapporo, Japan*

[f]*Environmental Organic Chemistry Laboratory, Chemistry Division, Atomic Energy Centre, Bangladesh Atomic Energy Commission, Dhaka 1000, Bangladesh*

[g]*Nuclear Safety, Security and Safeguards Division, Bangladesh Atomic Energy Commission, Dhaka 1207, Bangladesh*

[h]*Materials Science Division, Atomic Energy Centre, Bangladesh Atomic Energy Commission, Dhaka 1000, Bangladesh*

can act as a reducing agent as well as a stabilizer and thus enhance the rate of reduction and stabilization of the NPs.[18]

As an important component in the development of nanotechnology, NPs have been extensively explored for possible medical applications. Magnetic nanoparticles are considered to be more effective for bio-medical applications. NPs provide a particularly useful platform and demonstrate unique properties with potentially wide-ranging therapeutic applications.[19] Antibiotic resistant bacterial strains with different mechanisms are continually being found and thus new drugs are required.[20] Therefore, the finding of new antimicrobial agents with novel mechanisms of action is essential and is being extensively pursued in antibacterial drug discovery.[21] Recently, it has been demonstrated that metal oxide NPs exhibit excellent biocidal and biostatic actions against Gram-positive and Gram-negative bacteria.[22] Several reports are available for the synthesis of TiO_2 NPs using plant/leaf extracts of *Nyctanthes arbor-tristis*, *Solanum trilobatum*, *Annona squamosa*, *Catharanthus roseus*, *Calotropis gigantea*, and *Jatropha curcas*.[23–28]

In the present study, *Artocarpus heterophyllus* leaf extract was used as a reducing and surface modifying agent. To the best of our knowledge, this is the first report where *Artocarpus heterophyllus* leaf aqueous extract was used as a reducing and surface modifying agent in the synthesis of TiO_2 NPs. *Artocarpus heterophyllus*, commonly known as jackfruit, belongs to the Moraceae family and is widely cultivated and grows in the tropical regions of the world.[29] Consequently, the effect of bio-synthesized TiO_2 NPs was investigated against different types of human pathogens. Moreover, their cytotoxicity was investigated by applying them to two types of cell line: human carcinoma cells (HeLa) and normal cells (Vero) in order to find out about their anticancer activity and toxicity threshold limit, respectively.

Materials and methods

Materials

Artocarpus heterophyllus (jackfruit) leaves were collected locally from Dhaka, Bangladesh. Titanium(IV) isopropoxide (TTIP) was purchased from Merck, India. Bactotrypton, bacto agar, and yeast extract were purchased from Difco Laboratories (Detroit, MI, USA) and sodium chloride from the Wako Pure Chemical Company (Osaka, Japan). HeLa cell and Vero cell lines were obtained from the American type culture collection (USA and Canada). Dulbecco's modified Eagle's medium (DMEM) was purchased from Sigma (St. Louis, MO, USA). Fetal bovine serum was purchased from Biosera (Kansas City, MO, USA). Trypan blue stain solution (4%) was purchased from Bio-Rad (Hercules, CA, USA). All other chemicals and reagents were of analytical grade.

Synthesis of TiO_2 nanoparticles

The collected leaves were gently washed with de-ionized water to remove the dust and then sun-dried for about 10 days under dust-free conditions. Then the dried leaves were ground and sieved to get the finest powder. 10 g of the powdered leaves were mixed with 500 mL of de-ionized water and heated to 100 °C for 30 min and cooled to room temperature. The mixture was then filtered through Whatman no. 1 filter paper and the filtrate termed here as leaf extract was stored at 4 °C for further experiments. The leaf extract was added drop-wise into 0.5 M TTIP solution at a ratio of 4 : 1 under constant magnetic stirring at 100 °C. Then the room temperature cooled mixture was washed repeatedly with de-ionized water and centrifuged in order to remove the impurities. The obtained sample was dried at 105 °C in a hot air oven and finally calcined at 650 °C for 3 h.

Characterization of TiO_2 nanoparticles

The optimum calcination temperature for the formation of nano TiO_2 anatase phase was obtained from a thermogravimetric analysis, which was carried out under an N_2 atmosphere using a TA instrument (SDR Q-600) operating from 25° to 800 °C with a heating rate of 10°C min^{-1}. The elemental analysis of the sample was obtained from energy dispersive X-ray (EDX) spectroscopy measurements, performed by a JEOL JSM 7600 F instrument (Japan), using an acceleration voltage of 15 kV and an emission current of 12 μA. In order to analyze the functional groups in the leaf extract, which can act as reducing and surface modifying agents, their presence was confirmed by Fourier transform – infrared (FT-IR) analysis using a JASCO-FTIR-6300 instrument (Japan) on KBr pellets. 1% (w/w) samples were mixed with KBr powder and pressed into a sheer slice. FT-IR analysis of the sample was also carried out in order to confirm the formation of TiO_2 with surface modification. The crystalline phase was assessed by an X-ray powder diffractometer (Philips PANalytical X'PERT PRO) equipped with CuK_α radiation (1.5418 Å). The surface morphology was monitored by field emission scanning electron microscopy using a JEOL model JSM 7600 F instrument (Japan), applying an acceleration voltage of 15 kV and an emission current of 12 μA. The particle size was calculated from the transmission electron microscopy (TEM) analysis using a JEOL JEM 2010 instrument (Japan) recorded at an accelerating voltage of 120 kV. The magnetic property of the TiO_2 NPs was evaluated using a Vibrating Sample Magnetometer (EV-9 MicroSense, German).

Antibacterial activity of TiO_2 NPs

The antibacterial activity of the TiO_2 NPs was evaluated by considering four types of bacteria: *Escherichia coli* (ATCC 25922), *Salmonella typhimurium* (ATCC 14028), *Staphylococcus aureus* (ATCC 12228), and *Bacillus subtilis* (ATCC 14579) following the disc diffusion method described elsewhere.[29] Briefly, bacteria were cultured in Luria Broth (LB) medium (tryptone 1.5%, yeast extract 0.75%, sodium chloride 1.2%) in a 60 rpm shaking water bath at 37 °C. Then, 50 μL of bacterial medium was poured onto a Petri plate and smoothly smeared by a glass rod. 7 mm sized sterilized filter papers were soaked in 15 μL of TiO_2 NP suspension and placed on a culture plate for 24 h. Deionized water discs and commercial antibiotic discs were used as negative and positive controls, respectively.

Cytotoxicity of TiO_2 NPs

The cytotoxicity of the TiO_2 NPs was assessed from a cell viability experiment following a Trypan blue exclusion assay.[30]

The cells were cultured in DMEM medium supplemented with 10% FBS in a humidified incubator at 37 °C with 5% CO_2 in 25 cm^2 culture flasks. Then, the TiO_2 NPs were added into the flasks, and incubated for 48 h. In every treatment, fresh medium was added prior to treatment. After 48 h, the cell viability was measured using a Bio-Rad automated cell counter (Hercules CA, USA). Cell viability was expressed as a percentage of the total cell counts against the stained cell counts. Each experiment was performed at least three times to ensure reproducibility and statistical validity.

Results and discussion

The temperature-dependent weight losses of the sample using TGA have been shown in Fig. 1. The slope of the TG curve indicates that the weight losses of the studied sample could be clearly seen at different stages up to 650 °C. About 7% weight loss was noticed up to 100 °C, which is related to the release of water molecules attached to the surface of the synthesized sample. Weight loss up to 350 °C occurs due to the release of unreacted organic molecules present in the sample. Then the weight loss up to 550 °C is attributed to both the decomposition of the residual biomolecules and the crystallization of the sample. Sharp changes in weight loss from the TG plot were observed from 550 °C to 650 °C which were attributed to the condensation of the anatase phase of TiO_2.[31] Based on this result, 650 °C was selected as the calcination temperature for the synthesis of TiO_2 NPs.

The EDX spectra show two intense peaks at 4.51 and 0.53 keV corresponding to the presence of Ti and O, respectively (Fig. 2). The atomic percentages of Ti and O were 32 and 43, respectively, indicating the formation of non-stoichiometric TiO_2 with oxygen vacancies, which leads to better photocatalytic activity.[32] Two less intense peaks obtained at 0.28 and 0.39 keV are assigned as C and N, respectively. These impure elements originated from the leaf extract and depict their conjunction with the synthesized TiO_2 NPs.[29]

The FT-IR spectra of *A. heterophyllus* leaf powder are shown in Fig. 3a. The spectra clearly demonstrate that three strong peaks appeared at 3768, 3693 and 3435 cm^{-1}, corresponding to N–H stretching of amide, –OH stretching vibration (phenolic compounds), and –OH stretching of water, and other intense peaks appeared at 2924 and 2856 cm^{-1}, corresponding to the C–H stretching vibration and alkynes (flavonoids) which were reported as active reducing and capping agents.[33–35]

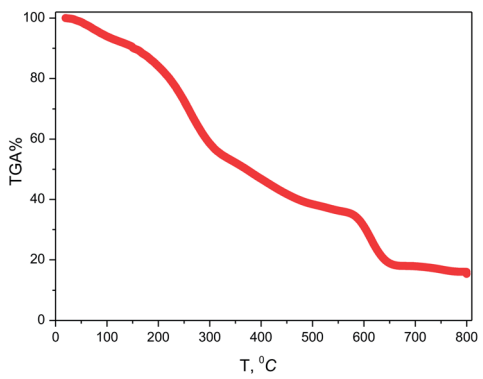

Fig. 1 TGA plot of TiO_2 NPs synthesized using *Artocarpus heterophyllus* leaf extract and $Ti[OCH(CH_3)_2]_4$ solution.

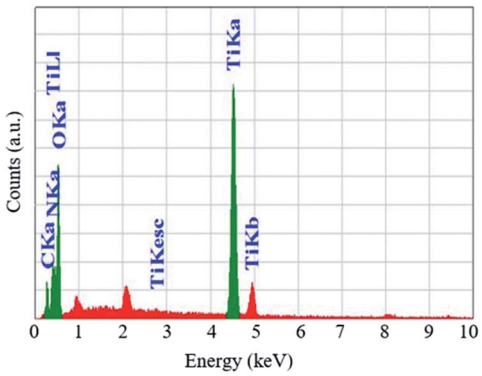

Fig. 2 EDX spectra of TiO_2 NPs and bioorganic components of *Artocarpus heterophyllus* leaf extract.

The details of peaks appearing for *A. heterophyllus* leaf powder and synthesized TiO_2 NPs are summarized in Table 1. Fig. 3b demonstrates that peaks almost similar to those of leaf powder appeared for synthesized TiO_2 NPs at 3757, 3693, 3435, 2926, 2858, 1624, and 1433 cm^{-1}. This observation implies that the peaks correspond to the biomolecules acting as capping and

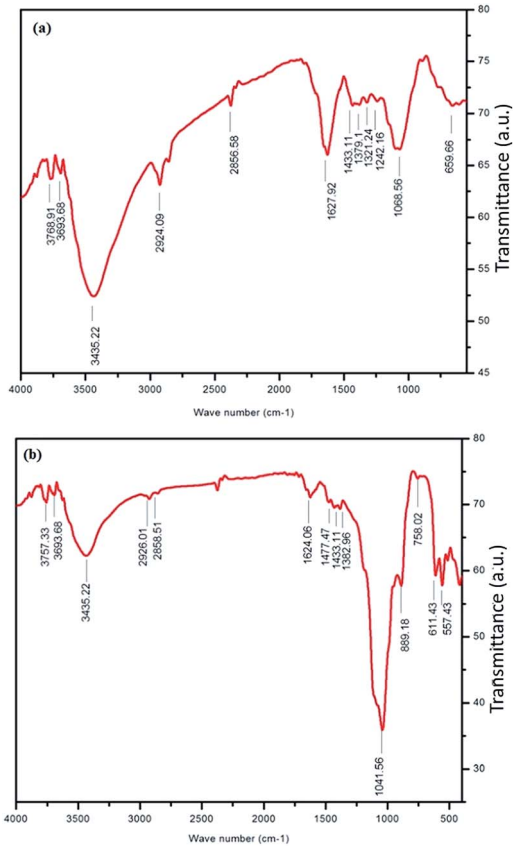

Fig. 3 FT-IR spectra of (a) *A. heterophyllus* (AH) leaf powder and (b) TiO_2 NPs indicating the conjugation of biomolecules with TiO_2 NPs obtained from AH leaf extract.

Table 1 Summary of FT-IR interpretation of *A. heterophyllus* leaf powder and TiO_2 NPs

Wavenumber (cm^{-1})			
A. heterophyllus leaf powder	TiO_2 NPs	Corresponding functional groups	References
3768	3757	N–H stretching of amide and –OH stretching vibration (phenolic compounds)	33 and 34
3693	3693		
3435	3435	O–H stretching of water molecule	12
1627	1624	O–H bending of water molecule	3
2924	2926	C–H stretching vibration and alkynes (flavonoids)	33 and 34
2856	2858		
1433	1433	Symmetric bending of $–CH_3$	35
—	1041	Si–O–Si stretching of silica	36
—	557	Bending vibration of Ti–O–Ti and Ti–O	33

stabilizing agents in TiO_2 NPs.[29] Moreover, two additional strong peaks observed at 557 and 1041 cm^{-1} in Fig. 3b are due to the vibration of Ti–O–Ti and Si–O–Si, respectively.[33,36] The vibration band of Ti–O–Ti firmly proves the formation of TiO_2 NPs.

It is important to note that the intensity of the almost similar peaks appearing for leaf powder and TiO_2 NPs was found to decrease in the TiO_2 NPs sample. Another peak with the highest intensity appearing for TiO_2 NPs, corresponding to the Si–O–Si stretching vibration, might be due to the presence of silica. Probably the leaf extract contains silicon which becomes silica after calcination. This residual silica might be responsible for the stability of TiO_2 NPs, which agrees well with the TG analysis.

The inspection of the XRD data was first carried out by the phase identification method. This procedure helped us to determine the presence of the mixed phase of TiO_2. We refined the XRD patterns using the FullProf program in profile matching mode.[37] Fig. 4 shows the refinement of the *Artocarpus heterophyllus* leaf extract mediated synthesized mixed phase of TiO_2. We found better fitting of the refinement using the cell parameters of anatase and panguite type mixed phase. We refined the XRD patterns using the reported cell parameters of anatase[38] and panguite[39] phases. Although several research groups reported the different phases of TiO_2 performing different synthesis conditions, the panguite phase is reported as a mixed metallic phase by Ma *et al.*[39] According to their reports, this mixed metallic phase is one of the oldest materials in the solar system and is formed by condensation. The highest intensity peak (Fig. 4) of the panguite phase near 33° is very small compared with the main phase, which implies that a small amount of panguite phase is synthesized as an impurity. This mixed phase might originate from the use *Artocarpus heterophyllus* leaf extract in the synthesis of TiO_2 NPs. The unit cell parameters, space group and *R* factor are summarized in Table 2 using two-phase model-based profile matching refinement.

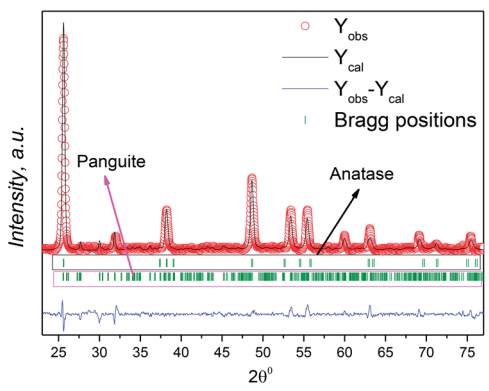

Fig. 4 Refined XPRD profiles of *Artocarpus heterophyllus* leaf extract mediated synthesized mixed phase TiO_2 NPs. The open red circles, black lines, the bottom blue line, and green vertical bars represent the experimental data, calculated pattern, difference curves, and Bragg positions, respectively.

Fig. 5a shows the FESEM image of the synthesized TiO_2 NPs with a high degree of crystallinity in which the surface morphology is found to be uniformly distributed with nano dimensions. The TEM image (Fig. 5b) clearly demonstrates that the synthesized TiO_2 NPs are spherical in shape with smooth edges and are uniformly distributed. The particle sizes of the synthesized TiO_2 NPs are in the approximate range of 15 to 20 nm, which is in good agreement with the crystallite size (15 nm) calculated using the XRD patterns. An intense look at the TEM image reveals that surface modification of the synthesized TiO_2 NPs was also obtained. The synthesized TiO_2 NPs are found to be less agglomerated, which might be due to the presence of biomolecule content capping agents on the surface of the TiO_2 NPs, as evidenced from the FT-IR and EDX analyses. It is worth mentioning here that the capping is found to be present even when the materials are calcined at high temperature, indicating their high temperature stability.

Room-temperature VSM measurement of our studied TiO_2 NPs is represented in Fig. 6. This figure demonstrates that the studied TiO_2 NPs have a very weak ferromagnetic nature at room temperature. Fig. 6 (inset) shows an enlarged view of the hysteresis loop obtained from VSM measurement at room temperature. These types of materials have been reported as diluted magnetic semiconductors with a room-temperature ferromagnetism nature, and are interesting materials for spintronic applications.[40] Although the origin of the magnetic behaviour is not clear, shallow defects, such as oxygen vacancies, might be the reason for the dilute ferromagnetic nature.[41] It has been established that magnetic nanoparticles are among promising materials for medical applications. So, the magnetic measurements fulfilled our aim towards the study of dilute ferromagnetic TiO_2 NPs.

Table 2 The unit cell parameters and volume *R*-factors refined by the profile matching method for the *Artocarpus heterophyllus* leaf extract mediated synthesized mixed phase TiO_2 NPs

		Unit cell parameters			Cell volume	Reliability factors	
Phase	Space group	*a*, Å	*b*, Å	*c*, Å	*V*, Å^3	R_B %	R_f %
Anatase	$I4_1/amd$	3.74232	3.74232	9.42118	131.943	0.777	0.782
Panguite	*Pbca*	9.49192	9.77530	9.93117	921.477	6.88	3.56

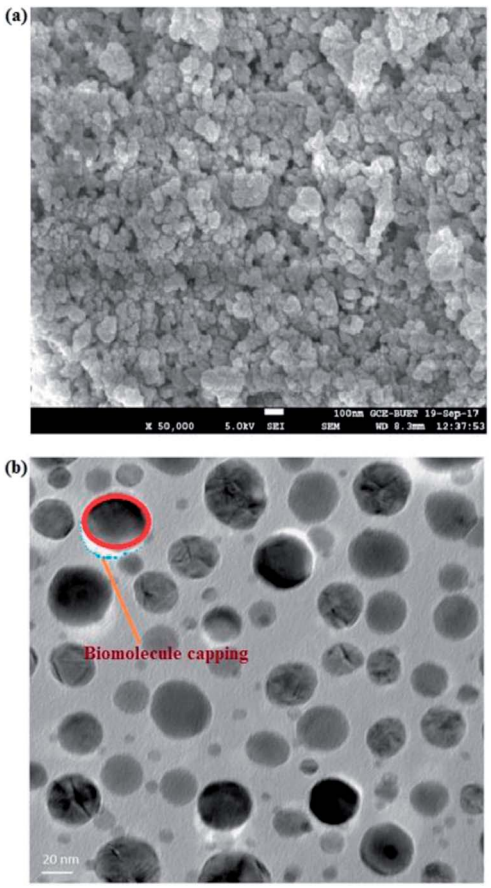

Fig. 5 (a) FESEM image and (b) TEM image of TiO_2 NPs synthesized using *A. heterophyllus* leaf extract and $Ti[OCH(CH_3)_2]_4$ solution.

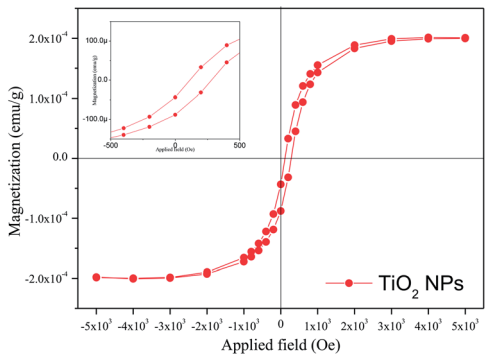

Fig. 6 The room-temperature magnetization curve of TiO_2 NPs synthesized using *A. heterophyllus* leaf extract and $Ti[OCH(CH_3)_2]_4$ solution. The inset shows an enlarged view of the hysteresis loop.

The antibacterial activity of green synthesized TiO_2 NPs surface modified by *Artocarpus heterophyllus* leaf extract was investigated against both Gram-negative (*E. coli* and *S. typhimurium*) and Gram-positive (*S. aureus* and *B. subtilis*) bacteria using an agar well diffusion assay. The observed zones of inhibition corresponding to experimental bacteria are shown in Fig. 7. However, the negative control (deionized water) did not show any zone of inhibition and the positive control (ampicillin) exhibited antibacterial activity against the four investigated human pathogens. Furthermore, the leaf extract used for the surface modifying agent of TiO_2 NPs was also exposed on the two types of bacteria, where no zone of inhibition was found, confirming the antibacterial activity of TiO_2 NPs. The antibacterial activity of the sample was compared with the other bio-synthesized TiO_2 NPs and is summarized in Table 3. The results clearly demonstrate that the efficiency of the currently studied *Artocarpus heterophyllus* leaf extract surface modified TiO_2 NPs has potential antibiotic activity against both Gram-positive and Gram-negative bacteria.

The antibacterial activity of surface modified TiO_2 NPs is supposed to be achieved through multiple mechanisms of phytochemicals and TiO_2 NPs. It is assumed that the phytochemicals are capable of binding with the bacterial cell wall and then penetrating into the bacterial cells.[42] In the course of time, TiO_2 NPs act as a catalyst to inactivate the enzymes of microorganisms that resist metabolism by interacting with the thiol groups of proteins, disrupting bacterial membranes and also affecting DNA replication.[42] The TiO_2 NPs are reported as being more effective material against Gram-negative bacteria than against Gram-positive bacteria because of the rigid, thick, multiple layers of peptidoglycan in the cell walls of Gram-positive bacteria preventing the nanoparticles from entering into the cell wall.[43]

The synthesized TiO_2 NPs were applied to HeLa cells and Vero cells with different concentrations of NPs starting from 1 mg L^{-1} to 5000 mg L^{-1} and the cell viability was measured for cytotoxicity assessment. The phase contrast microscopic images of TiO_2 NP induced cytomorphological changes and growth inhibition of two cell lines with control, leaf extract and at different concentrations of TiO_2 NPs are shown in Fig. 8.

The cell viability indicates that the synthesized TiO_2 NPs are not toxic against the two selected cell lines up to 1000 mg L^{-1}. This result implies that our synthesized TiO_2 NPs could be used for various applications with concentrations up to 1000 mg L^{-1} without any toxicity. The synthesized TiO_2 NPs at 2000 mg L^{-1}

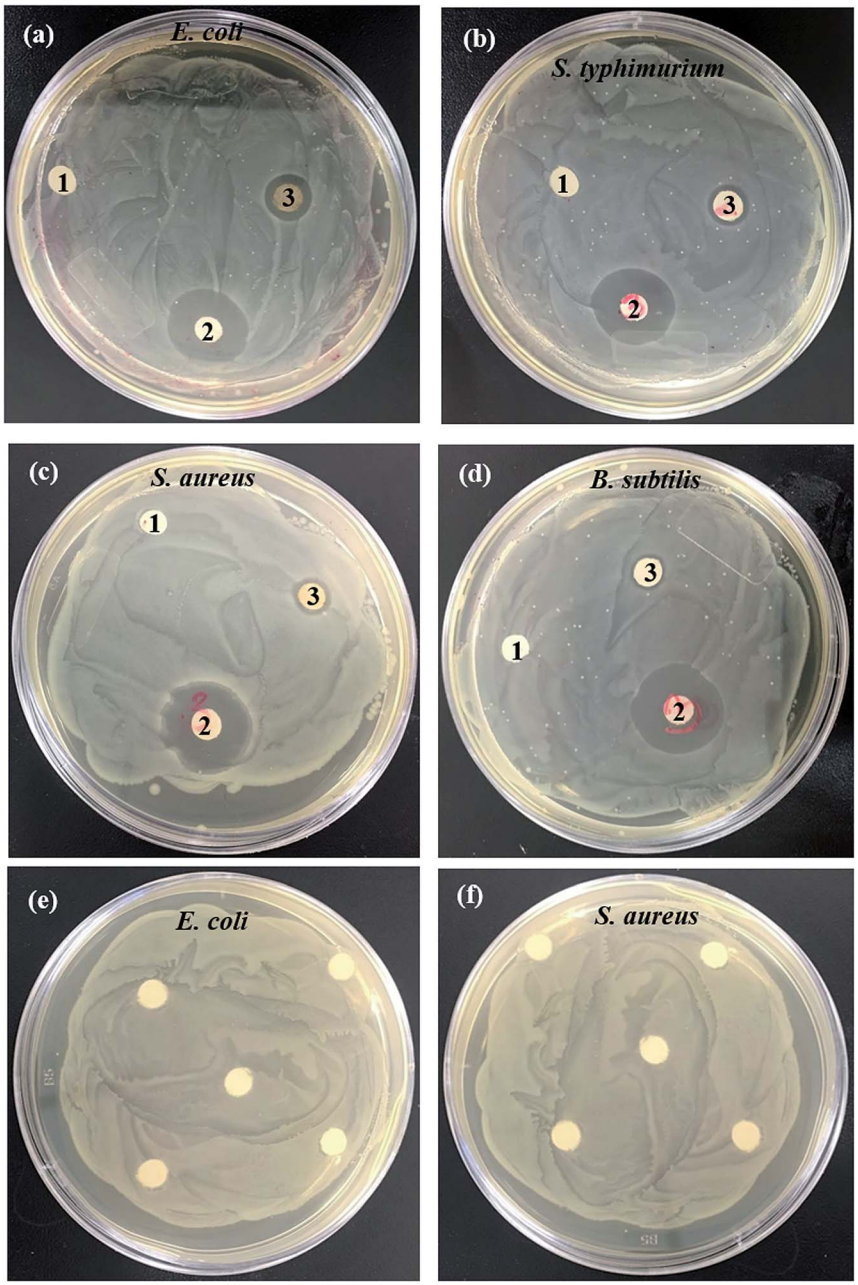

Fig. 7 Antibacterial activity of 1 deionized water, 2 ampicillin and 3 TiO_2 NPs against Gram-negative (a) *E. coli* and (b) *S. typhimurium*, and Gram-positive (c) *S. aureus* and (d) *B. subtilis* pathogenic bacteria; (e, f) exposure of leaf extract against *E. coli* and *S. aureus*.

are found to be toxic with a decrease in cell viability of around 10% against the carcinoma HeLa cell line, but the same concentration of TiO_2 NPs does not affect activity against the Vero cell line. In the case of the Vero cell line, the synthesized TiO_2 NPs showed toxicity at a dose of 3000 mg L^{-1}. The cell viability is found to decrease with an increase in concentration for both cell lines. In order to confirm whether the toxicity arose from the TiO_2 NPs or the leaf extract, *Artocarpus heterophyllus* aqueous leaf extract was further applied to both cell lines. For the treatment with leaf extract there was no change in cell viability observed in comparison to the control, indicating that TiO_2 NPs were responsible for the cytotoxicity. Although the cytotoxicity of TiO_2 NPs has been investigated extensively, the precise mechanisms where TiO_2 NPs induce cell death are mostly unclear, as the cytotoxicity varies from cell to cell as well as from NPs to NPs.[47] The cytotoxic effect of TiO_2 NPs is mainly due to the disruption of the antioxidant system.[48] Thus, oxidative stress increases the consequences of cellular-level oxidative stress in free radical mediated membrane damage, including mitochondrial and plasma membranes, which results in damage to cellular protein, lipids and DNA and finally leads to cell death and dysfunction of the electronic chain.[48] The

Table 3 Various phyto-synthesized TiO_2 NP induced zones of inhibition against different harmful human pathogenic bacteria

Name of various pathogenic bacteria	Extracted substances	Concentrations of TiO_2 NPs (mg L^{-1})	Zone of inhibition (mm)	References
E. coli	*M. citrifolia*	100	9	33
	A. flavus	40	35	44
	A. heterophyllus	100	23	Present work
S. typhimurium	*A. niger*	40	18	45
	A. heterophyllus	100	20	Present work
S. aureus	*M. citrifolia*	100	12	33
	A. flavus	40	25	44
	H. rosa-sinensis	20	11	46
	A. heterophyllus	100	17	Present work
B. subtilis	*M. citrifolia*	100	10	33
	A. flavus	45	22	44
	A. niger	40	17	45
	A. heterophyllus	100	15	Present work

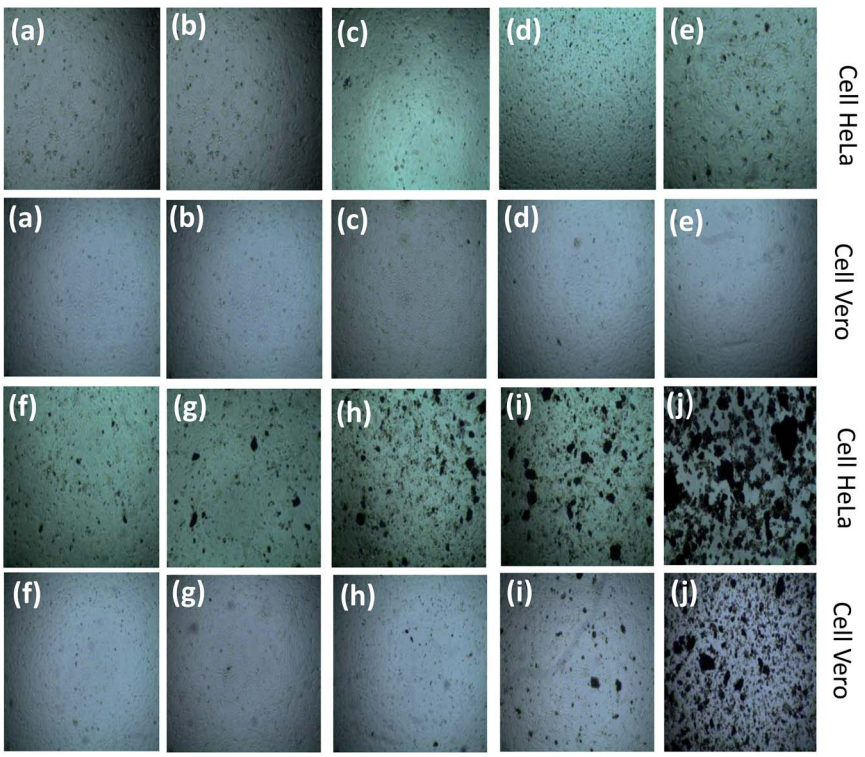

Fig. 8 Phase contrast microscopic images of TiO_2 NP induced cytomorphological changes and growth inhibition of HeLa and Vero cell lines with controls and at different concentrations: (a) control, (b) leaf extract, (c) 20 mg L^{-1}, (d) 50 mg L^{-1}, (e) 100 mg L^{-1}, (f) 500 mg L^{-1}, (g) 1000 mg L^{-1}, (h) 2000 mg L^{-1}, (i) 3000 mg L^{-1}, and (j) 5000 mg L^{-1}.

cytotoxicity observed in the present study could be due to oxidative stress-mediated cellular damage.

Conclusions

The low-cost, surface modified, green synthesis of TiO_2 NPs was investigated for antibiotic application and *in vitro* cytotoxicity. The synthesized TiO_2 NPs were oxygen non-stoichiometric and surface modified. The dilute ferromagnetic nature of the sample at room temperature fulfilled the criteria of highly efficient materials for biomedical application. The application of *Artocarpus heterophyllus* leaf extract surface modified TiO_2 NPs against both Gram-positive and Gram-negative bacteria and their comprehensive studies in the literature concluded that the current sample has potential antibiotic activity. The toxicity investigation of surface modified TiO_2 NPs allow them to be used for various applications with concentrations up to 1000 mg L^{-1}. The study of the current sample with HeLa cells implies that this material could be used as an anticancer agent at a concentration of 2000 mg L^{-1}.

Conflicts of interest

The authors declare no conflict of interest.

Acknowledgements

The authors would like to thank the Nanoscience and Technology Research Laboratory and Materials Science Division, Atomic Energy Centre, Dhaka, and Centre for Advance Research in Science, University Dhaka, Dhaka, Bangladesh for providing assistance regarding synthesis and characterization of the samples.

Notes and references

1 Y. Li, T. J. White and S. H. Lim, *J. Solid State Chem.*, 2004, **177**, 1372–1381.
2 N. I. A. Salim, S. A. Bagshaw, A. Bittar, T. Kemmtt, A. J. Mcquillan, A. M. Mills and M. J. Ryan, *J. Mater. Chem.*, 2000, **10**, 2358–2363.
3 S. Ito, S. Inoue, H. Kawada, M. Hara, M. Iwaski and H. Tada, *J. Colloid Interface Sci.*, 1999, **216**, 59–64.
4 C. J. Barbe, F. Arendse, P. Comte, M. Jirousek, F. Lenzmann, V. Shklover and M. Gratzel, *J. Am. Ceram. Soc.*, 1997, **80**, 3157–3171.
5 S. Monticone, R. Tufeu, A. V. Kanaev, E. Scolan and C. Sanchez, *Appl. Surf. Sci.*, 2000, **162**, 565–570.
6 S. Boujday, F. Wunsch, P. Portes, J. F. Bocquet and C. C. Justin, *Sol. Energy Mater. Sol. Cells*, 2004, **83**, 421–433.
7 O. Carp, C. L. Huisman and A. Reller, *Prog. Solid State Chem.*, 2004, **32**, 33–177.
8 A. M. Ruiz, G. Sakai, A. Cornet, K. Shimanoe, J. R. Morante and N. Yamazoe, *Sens. Actuators, B*, 2004, **103**, 312–317.
9 H. Shi, R. Magaye, V. Castranova and J. Zhao, *Part. Fibre Toxicol.*, 2013, **10**, 15.
10 N. Roy, Y. Park, Y. Sohn, K. T. Leung and D. Pradhan, *ACS Appl. Mater. Interfaces*, 2014, **6**, 16498–16507.
11 K.-S. Lin, H.-W. Cheng, W.-R. Chen and J.-F. Wu, *J. Environ. Eng. Manage.*, 2010, **20**, 69–76.
12 A. K. M. A. Ullah, A. K. M. F. Kibria, M. Akter, M. N. I. Khan, M. A. Maksud, R. A. Jahan and S. H. Firoz, *J. Saudi Chem. Soc.*, 2017, **21**, 830–836.
13 A. Hossain, S. Roy and K. Sakthipandi, *Ceram. Int.*, 2019, **45**, 4152–4166.
14 A. K. M. A. Ullah, A. K. M. F. Kibria, M. Akter, M. N. I. Khan, A. R. M. Tareq and S. H. Firoz, *Water Conservation Science and Engineering*, 2017, **1**, 249–256.
15 S. M. Gupta and M. Tripathi, *Cent. Eur. J. Chem.*, 2012, **10**, 279–294.
16 M. A. A. Mamun, M. Noor, A. K. M. A. Ullah, M. S. Hossain, M. A. Matin, F. Islam and M. A. Hakim, *Mater. Res. Express*, 2019, **6**, 016102.
17 A. Mbonyiryivuze, S. Zongo, A. Diallo, S. Bertrand, E. Minani, L. L. Yadav, B. Mwakikunga, S. M. Dhlamini and M. Maaza, *Phys. Mater. Chem.*, 2015, **3**, 12–17.
18 K. S. Kavitha, B. Syed, D. Rakshith, H. U. Kavitha, H. C. Y. Rao, B. P. Harini and S. Satish, *Int. Res. J. Biol. Sci.*, 2013, **2**, 66–76.
19 X. Gao, Y. Cui, R. M. Levenson, L. W. Chung and S. Nie, *Nat. Biotechnol.*, 2004, **22**, 969–976.
20 J. M. Streit, T. R. Fritsche, H. S. Sader and R. N. Jones, *Diagn. Microbiol. Infect. Dis.*, 2004, **48**, 137–143.
21 A. Coates, Y. Hu, R. Bax and C. Page, *Nat. Rev. Drug Discovery*, 2002, **1**, 895–910.
22 T. M. L. Goerne, M. A. A. Lemus, V. A. Morales, E. G. Lopez and P. C. Ocampo, *J. Nanomed. Nanotechnol.*, 2012, **S5**, 003.
23 M. Thamima and S. Karuppuchamy, *Adv. Sci., Eng. Med.*, 2014, **6**, 1–8.
24 G. Rajakumar, A. A. Rahuman, C. Jayaseelan, T. Santhoshkumar, S. Marimuthu, C. Kamaraj, A. Bagavan, A. A. Zahir, A. V. Kirthi, G. Elango, P. Arora, R. Karthikeyan, S. Manikandan and S. Jose, *Parasitol. Res.*, 2014, **113**, 469–479.
25 K. Velayutham, A. Rahuman, G. Rajakumar, T. Santhoshkumar, S. Marimuthu, C. Jayaseelan, A. Bagavan, A. Kirthi, C. Kamaraj, A. A. Zahir and G. Elango, *Parasitol. Res.*, 2012, **111**, 2329–2337.
26 R. B. Malabadi, R. K. Chalannavar, N. T. Meti, G. S. Mulgund, K. Nataraja and S. V. Kumar, *Res. Pharm.*, 2012, **2**, 18–31.
27 S. Marimuthu, A. A. Rahuman, C. Jayaseelan, A. V. Kirthi, T. Santhoshkumar, K. Velayutham, A. Bagavan, C. Kamaraj, G. Elango, M. Iyappan, C. Siva, L. Karthik and K. V. B. Rao, *Asian Pac. J. Trop. Dis.*, 2013, **6**, 682–688.
28 A. C. Nwanya, P. Ugwuoke, P. M. Ejikeme, E. O. Oparaku and F. I. Ezema, *Int. J. Electrochem. Sci.*, 2012, **7**, 11219–11235.
29 A. K. M. A. Ullah, M. F. Kabir, M. Akter, A. N. Tamanna, A. Hossain, A. R. M. Tareq, M. N. I. Khan, A. K. M. F. Kibria, M. Kurasaki and M. M. Rahman, *RSC Adv.*, 2018, **8**, 37176–37183.
30 M. Akter, M. M. Rahman, A. K. M. A. Ullah, M. T. Sikder, T. Hosokawa, T. Saito and M. Kuasaki, *J. Inorg. Organomet. Polym. Mater.*, 2018, **28**, 1483–1493.
31 Y. Yang, X. Wang and L. Li, *J. Am. Ceram. Soc.*, 2008, **91**, 632–635.
32 G. Liu, H. G. Yang, X. Wang, L. Cheng, H. Lu, L. Wang, G. Q. Lu and H. M. Cheng, *J. Phys. Chem.*, 2009, **113**, 21784–21788.
33 M. Sundrarajan, K. Bama, M. Bhavani, S. Jegatheeswaran, S. Ambika, A. Sangili, P. Nithya and R. Sumathi, *J. Photochem. Photobiol., B*, 2017, **171**, 117–124.
34 P. Kalainila, V. Subha, R. S. E. Ravindran and S. Renganathan, *Asian J. Pharm. Clin. Res.*, 2014, **7**, 39–43.
35 R. Begum, M. G. Aziz, M. B. Uddin and Y. A. Yusof, *Agriculture and Agricultural Science Procedia*, 2014, **2**, 244–251.
36 H. Fu, X. Ding, C. Ren, W. Li, H. Wu and H. Yang, *RSC Adv.*, 2017, **7**, 16513–16523.
37 J. R. Carvajal, *Phys. B*, 1993, **192**, 55–69.
38 Q. Xu, J. Yu, J. Zhang, J. Zhang, J. Zhang and G. Liu, *Chem. Commun.*, 2015, **51**, 7950–7953.
39 C. Ma, O. Tschauner, J. R. Beckett, G. R. Rossman and W. Liu, *Am. Mineral.*, 2012, **97**, 1219–1225.

40 Y. Matsumoto, M. Murakami, T. Shono, T. Hasegawa, T. Fukumura, M. Kawasaki, P. Ahmet, T. Chikyow, S. Koshihara and H. Koinuma, *Science*, 2001, **291**, 854–856.
41 Z. M. Tian and S. L. Yuan, *Effects of sintering temperature and atmosphere on magnetism in Mn-doped TiO_2 bulk samples*, Department of Physics, Huazhong University of Science and Technology, Wuhan 430074, PR China, 2007.
42 L. Kvitek, A. Panacek, J. Soukupova, M. Kolar, R. Vecerova and R. Prucek, *J. Phys. Chem. C*, 2008, **112**, S1005825–5834.
43 S. Ahmed, M. Ahmad, B. L. Swami and S. Ikram, *J. Adv. Res.*, 2016, **7**, 17–28.
44 G. Rajakumar, A. A. Rauman, S. M. Roopan, V. G. Khanna, G. Elango, C. Kamaraj, A. A. Zahir and K. Velayutham, *Spectrochim. Acta, Part A*, 2012, **91**, 23–29.
45 B. Durairaj, S. Muthu and T. Xavier, *Adv. Appl. Sci. Res.*, 2015, **6**, 45–48.
46 P. S. M. Kumar, A. P. Francis and T. Devasena, *Journal of Environmental Nanotechnology*, 2014, **3**, 78–85.
47 K. Soto, K. M. Garzal and E. Murr, *Acta Biomater.*, 2007, **3**, 351–358.
48 M. Aktera, M. T. Sikder, M. M. Rahmana, A. K. M. A. Ullah, K. F. B. Hossain, S. Banika, T. Hosokawa, T. Saito and M. Kurasaki, *J. Adv. Res.*, 2018, **9**, 1–16.